



HAL
open science

Non-leaky longitudinal acoustic modes in ScxAl1-xN/sapphire structure for high-temperature sensor applications

Thierry Aubert, Natalya Naumenko, Florian Bartoli, Philippe Pigeat, Jérémy Streque, Jaafar Ghanbaja, Omar Elmazria

► To cite this version:

Thierry Aubert, Natalya Naumenko, Florian Bartoli, Philippe Pigeat, Jérémy Streque, et al.. Non-leaky longitudinal acoustic modes in ScxAl1-xN/sapphire structure for high-temperature sensor applications. Applied Physics Letters, 2019, 115 (8), pp.083502. 10.1063/1.5114871 . hal-02272689

HAL Id: hal-02272689

<https://hal.science/hal-02272689>

Submitted on 28 Aug 2019

HAL is a multi-disciplinary open access archive for the deposit and dissemination of scientific research documents, whether they are published or not. The documents may come from teaching and research institutions in France or abroad, or from public or private research centers.

L'archive ouverte pluridisciplinaire **HAL**, est destinée au dépôt et à la diffusion de documents scientifiques de niveau recherche, publiés ou non, émanant des établissements d'enseignement et de recherche français ou étrangers, des laboratoires publics ou privés.

Non-leaky longitudinal acoustic modes in $\text{Sc}_x\text{Al}_{1-x}\text{N}$ /Sapphire structure for high-temperature sensor applications

Thierry Aubert^{*1,2}, Natalya Naumenko³, Florian Bartoli^{1,2,4}, Philippe Pigeat⁴, Jérémy
Streque⁴, Jaafar Ghanbaja⁴, Omar Elmazria⁴

¹*Laboratoire Matériaux Optiques, Photonique et Systèmes (LMOPS), CentraleSupélec, Université Paris-Saclay, Metz F-57070, France*

²*Université de Lorraine, Matériaux Optiques, Photonique et Systèmes (LMOPS), Metz F-57070, France*

³*National University of Science and Technology "MISIS", Moscow 119049, Russia*

⁴*Institut Jean Lamour, UMR 7198 Université de Lorraine–CNRS, Nancy 54000, France*

Abstract

Multilayered structures based on wide bandgap nitride piezoelectric thin films are very attractive for high-temperature surface acoustic waves (SAW) sensor applications. In this respect, scandium aluminium nitride (ScAlN) films are of particular interest as they combine enhanced piezoelectric properties and slower acoustic waves velocities when the Sc content steadily increases up to 40%. This property offers the possibility to combine slow ScAlN films on fast substrates like sapphire, to generate higher-order SAW modes which often show a better electromechanical coupling coefficient k^2 compared to zero-order modes. In this letter, we show that low-attenuated longitudinal SAW can be generated in $\text{Sc}_x\text{Al}_{1-x}\text{N}$ /Sapphire structure, for x parameter varying in a large range. This theoretical result is then confirmed by the experimental investigation of SAW resonators based on highly-textured (002) $\text{Sc}_{0.09}\text{Al}_{0.91}\text{N}$ films sputtered on c-cut sapphire substrates. It is finally shown that the use of electrodes based on metals with high density can lead to SAW structures offering a unique combination between a large bandgap over 5 eV, a k^2 value beyond 1% and a high SAW velocity near 10000 m/s.

* Corresponding author: thierry.aubert@centralesupelec.fr

Surface acoustic waves (SAW) devices are key components of modern telecommunication systems, including mobile phones. They are also widely investigated for sensor applications as they can be very sensitive to environmental parameters, including temperature, pressure, strain, etc. SAW sensors have in particular a great added value for high-temperature applications, as they are passive components, thus requiring neither embedded electronics, nor a power source to be wirelessly interrogated. Consequently, SAW technology can provide measurement solutions to several industrial sectors including metallurgy, aeronautics or petrochemicals, regarding the remote control of moving or poorly accessible parts placed in hot environments. Achievements of the last two decades led to wireless SAW resonators based on langasite ($\text{La}_3\text{Ga}_5\text{SiO}_{14}$; LGS) crystals, operable up to 650°C [1]. However, the sensing performance of LGS-based SAW sensors at higher temperatures is limited by low quality factors which result from oxygen ion transport and diffusion in the LGS lattice. This limitation could be overcome by the use of multilayered structures based on aluminum nitride films (AlN). Indeed, with a bandgap of 6.2 eV, the electrical resistivity of AlN at 1000°C remains several orders of magnitude higher than that of LGS at 600°C [2]. Several recent studies have shown that SAW sensors based on AlN/Sapphire bilayer structure could be used up to 1000°C [3-4]. However, the performances of this structure are limited by the relatively weak piezoelectric properties of AlN, leading to an electromechanical coupling coefficient k^2 of 0.3% at best [5]. Such a low value leads to large energy losses, thereby restraining harsh environment applications where every fragment of energy must be carefully preserved, especially so regarding passive technologies. Moreover, it prohibits the design of wideband devices, and thus ID-tag sensors based on the reflective delay lines technology [6].

However, Akiyama *et al.* showed in 2009 that it is possible to significantly increase the piezoelectric properties of AlN films by partially substituting aluminium atoms by scandium ones in the AlN crystal structure [7]. The piezoelectric properties of scandium aluminium nitride (ScAlN or $\text{Sc}_x\text{Al}_{1-x}\text{N}$) alloy films steadily strengthen with the scandium ratio as long as the latter does not exceed 43%. Above this ratio, the crystalline structure changes from wurtzite-like structure to the non-centrosymmetric rock salt structure in which ScN films crystallize. This improvement, intrinsic to ScAlN films, is amplified by two additional phenomena related to the whole bilayer structure. First, acoustic waves velocities in $\text{Sc}_x\text{Al}_{1-x}\text{N}$ films decrease with the Sc content [8]. As a result, acoustic modes propagating in ScAlN/Sapphire structure appear to be better confined in the film and

their piezoelectric coupling increases. Moreover, in bilayer structures constituted by a slow piezoelectric thin film over a fast non-piezoelectric substrate, the number of acoustic modes increases with the film thickness. Apart from zero-order modes (Rayleigh SAW and SH-polarized SAW) higher-order modes appear at certain film thicknesses. Some of these modes can exhibit much more coupling compared to zero-order modes. Additionally, these faster modes enable the design, for a given operating frequency, of thicker and wider IDT fingers for more robustness in harsh environments.

In the dispersion curve, the branches corresponding to these higher-order modes can arise from the slow shear, fast shear and longitudinal bulk acoustic waves (BAW) velocities of the substrate. In particular, the branch of quasi-longitudinal waves arises from BAW propagating with a velocity close to 12000 m/s for sapphire but such waves usually attenuate strongly because of BAW radiation into the substrate. However, it was shown that non-leaky solutions can exist on the longitudinal leaky SAW branch when sapphire substrate is combined with ZnO film [9]. In this letter, we demonstrate that low-attenuated longitudinal leaky waves can also exist in $\text{Sc}_x\text{Al}_{1-x}\text{N}/\text{Sapphire}$, more appropriate for high-temperature applications. The suitable conditions in order to generate SAW modes with high velocities are numerically studied. In particular, we show that low-attenuated waves can propagate with velocities in the range 9000-11000 m/s and $k^2 > 1\%$. This mode allows the design of high-frequency devices, for example 2.45 GHz ID-tag reflective delay lines with wavelengths as large as 4 μm . Moreover, it is demonstrated that such solutions can exist with parameter x varying in a wide range. This point is crucial as the bandgap of $\text{Sc}_x\text{Al}_{1-x}\text{N}$ films drops when parameter x increases, reaching 3.0 eV for $x = 0.3$ [10]. Consequently, we decided to focus our experimental efforts on $\text{Sc}_{0.1}\text{Al}_{0.9}\text{N}$ films, which offer a very good compromise. It allows the generation of low-attenuated high-velocity waves, while offering a large bandgap of 5.2 eV, suitable for high-temperature applications.

In [9] it was shown that high-velocity quasi-longitudinal leaky SAWs exist in ZnO/Sapphire structure and transform into non-leaky waves at certain points of the 2D space (θ, h_f) , where the angle θ determines the sapphire orientation and h_f is the film thickness. Similar non-attenuated longitudinal SAW solutions were previously found numerically in both diamond and silicon carbide (SiC) with ZnO films on top of them [9,11]. For ZnO/SiC the existence of high-velocity SAW (HVSAW) was confirmed experimentally [11]. Such waves can propagate in a low-velocity film deposited on a high-velocity substrate. They have specific one-partial structures and are located on the

leaky SAW branch arising from the longitudinal BAW propagating in the substrate. The existence conditions for HVSAWs, with requirements to combined substrate and film materials, were derived analytically in [12].

If a layered structure with a specific sapphire orientation is used as a substrate to achieve SAW resonators, a periodic metal grating with periodicity p is developed on top of it. Acoustic waves velocities depend on both electrode and film thicknesses, h_{EL} and h_f . In this case, the desired low attenuation of longitudinal leaky SAW can be achieved by the optimization of these two thicknesses, instead of the film thickness and substrate orientation.

The numerical procedure required for the search of the non-attenuated longitudinal solutions in the 2D space (h_f, h_{EL}) includes the simulation of admittance functions of SAW resonators and the extraction of complex velocities of leaky waves $V' = V^*(1 + j\delta)$ at each point of this space, where δ is the attenuation coefficient. If the velocities V_R and V_A refer, respectively, to the short-circuit (resonance) and open-circuit (anti-resonance) electrical conditions, the electromechanical coupling of the analyzed acoustic mode can be also estimated, as $k^2 \approx 2(V_A - V_R)/V_R$.

Fig. 1a shows the simulated velocities V_R of acoustic modes propagating in $Sc_{0.4}Al_{0.6}N/Sapphire$ with an Al grating on top, as functions of the film thickness. Simulations were made with the software SDA-FEM-SDA [13] using $Sc_{0.4}Al_{0.6}N$ constants reported in [14], when the Al thickness is $h_{Al} = 0.023\lambda$, where $\lambda = 2p$ is the wavelength. The velocities of Rayleigh SAW and SH-SAW modes start from 5490 m/s and 6531 m/s, respectively, when the film thickness is negligible and decrease with h_f while the coupling k^2 of Rayleigh SAW increases due to the better confinement of the wave in the piezoelectric film (**Fig. 1b**). The zero-order longitudinal mode was not observed in the analyzed structure. The first-order SH-SAW and longitudinal modes appear, respectively, at $h_f \approx 0.25\lambda$ and $h_f \approx 0.3\lambda$. They arise from the corresponding BAWs propagating in sapphire with velocities of 6766 m/s and 11147 m/s.

The longitudinal leaky SAW branch exists in a finite range of film thicknesses, with a velocity confined in the interval between the velocities of the longitudinal BAWs in sapphire and in $Sc_xAl_{1-x}N$. A growth in x widens this interval, and thus it is easier to find low-attenuated longitudinal waves within it. However, simulations revealed that low-attenuated longitudinal leaky waves can exist in $Sc_xAl_{1-x}N/Sapphire$ when the Sc content is much less than $x = 0.4$.

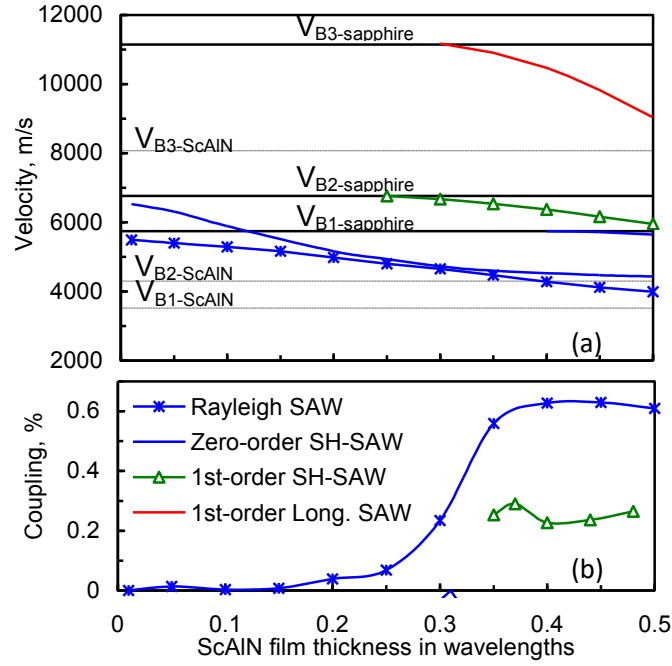


Fig. 1. Velocity and electromechanical coupling of acoustic modes propagating in $Sc_{0.4}Al_{0.6}N/Sapphire$ with Al grating, as functions of ScAlN thickness, when $h_{Al}=0.023\lambda$. V_{B1} , V_{B2} and V_{B3} refer to slow shear, fast shear and longitudinal BAW velocities respectively.

In order to confirm it experimentally, $Sc_{0.09}Al_{0.91}N$ thin films have been deposited on c-cut sapphire substrates by reactive magnetron sputtering, using a composite Al-Sc target. The actual composition of the films was revealed by energy dispersive X-ray spectroscopy. Several plasma parameters have been tested in order to obtain highly-textured ScAlN films, and thus optimize the piezoelectric properties. X-ray diffraction (XRD) measurements show that the optimized films are well oriented, with a rocking-curve value of 0.78° for the (002) XRD peak. This result is confirmed by transmission electron microscopy (TEM) and the associated selected area electronic diffraction (SAED) patterns (Fig. 2).

200 nm Al electrodes were then patterned using optical lithography, in order to achieve synchronous SAW resonators with a wavelength of $6.5 \mu m$, and SAW propagating along the X direction of the sapphire substrate. A low-attenuated wave propagating with a velocity of 10179 m/s was finally observed in a resonator based on $Sc_{0.09}Al_{0.91}N/Sapphire$ with $h_f = 0.425\lambda$, in addition to Rayleigh SAW ($V=4738$ m/s) and SH-SAW ($V=6662$ m/s) (Fig. 3a).

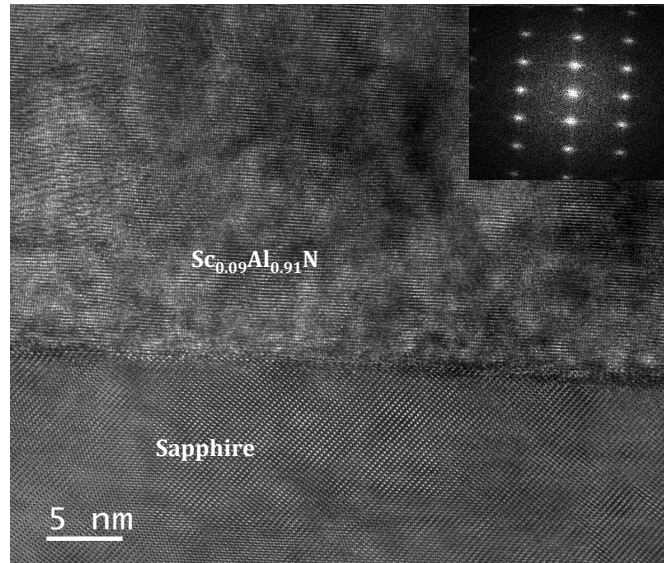


Fig. 2. TEM image and SAED pattern of optimized $\text{Sc}_{0.09}\text{Al}_{0.91}\text{N}$ film grown on sapphire

This device was then characterized at high temperatures, using an RF prober station (S-1160, Signatone Corp., Gilroy, CA) equipped with a thermal probing system that enables to control the device temperature up to 600 °C (S-1060, Signatone). Even if aluminium is not the most suitable metal for high-temperature measurements, the high-velocity SAW mode is still clearly visible at 575°C, confirming its relevance for the aimed application (Fig. 4).

The material constants of $\text{Sc}_{0.09}\text{Al}_{0.91}\text{N}$ have to be determined, but we were able to fit the simulated velocities of the two lower-velocity modes with their measured values, assuming a linear dependence of elastic constants on x , in the range between pure AlN and $\text{Sc}_{0.4}\text{Al}_{0.6}\text{N}$.

The simulated admittance obtained with these material constants is shown in Fig. 3b. The structure of the main modes is illustrated by colored diagrams, referred to the largest components of their polarization vectors \mathbf{u} (shear vertical u_3 for Rayleigh SAW, shear horizontal u_2 for SH SAW and longitudinal u_1 for high-velocity mode). Though the simulated velocity of the longitudinal mode was larger than the measured value, the analysis of the wave structure revealed a nearly pure longitudinal polarization. The wave resembles a plate mode, the energy being confined in the ScAlN film. However, further simulations showed that the longitudinal wave is not entirely localized in the film even when its attenuation coefficient tends to zero, and the acoustic energy stays distributed between the film and the substrate. Non-attenuated longitudinal waves with similar structure were recently found in a lithium tantalate plate bonded to a quartz substrate [15].

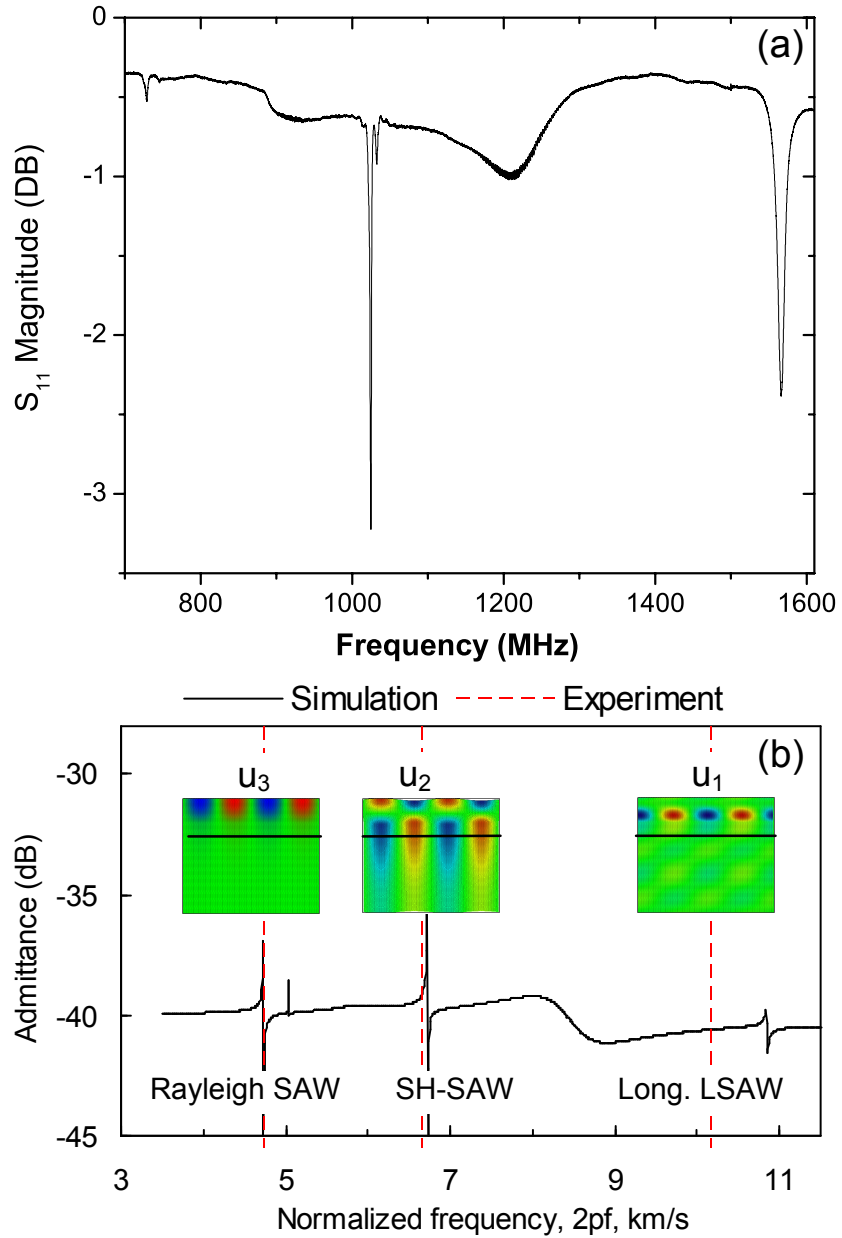


Fig. 3 (a) Experimental response of SAW resonators based on $Sc_{0.09}Al_{0.91}N/Sapphire$ structure (b) Simulated admittance of Al grating on $Sc_{0.09}Al_{0.91}N/Sapphire$ obtained with fitted constants, compared with experimental velocity values. The thicknesses of ScAlN and Al electrodes are $h_{ScAlN}=0.425\lambda$, and $h_{Al}=0.023\lambda$, respectively.

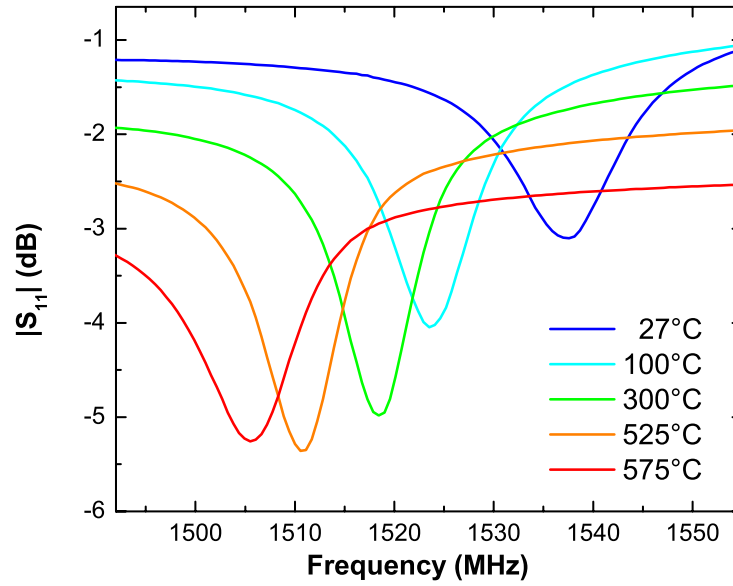


Fig. 4. High-temperature experimental characterization of the longitudinal SAW mode in $\text{Sc}_{0.09}\text{Al}_{0.91}\text{N}/\text{Sapphire}$.

Application of metals with higher density for the grating, instead of Al, may be useful to increase the reflectivity in SAW resonators and is more suitable for the intended applications in high-temperature environments, since such metals have often refractory properties. To check if the analyzed low-attenuated longitudinal modes still exist in $\text{Sc}_x\text{Al}_{1-x}\text{N}/\text{Sapphire}$ with other metals, simulations were made with Cu and Au gratings. The attenuation coefficient δ of high-velocity leaky SAW was extracted from simulated admittances of Cu gratings on $\text{Sc}_{0.4}\text{Al}_{0.6}\text{N}/\text{Sapphire}$, as a function of the film and electrode thicknesses. The results are shown in Fig. 5 and reveal the existence of a combination of optimal thicknesses that provide nearly zero attenuation coefficients. An example of simulated admittance function obtained with $h_f = 0.515 \lambda$ and $h_{\text{Cu}} = 0.05 \lambda$ is presented in Fig. 6. The longitudinal wave propagates with a velocity of about 9000 m/s, $k^2=0.58\%$ and has a negligible attenuation.

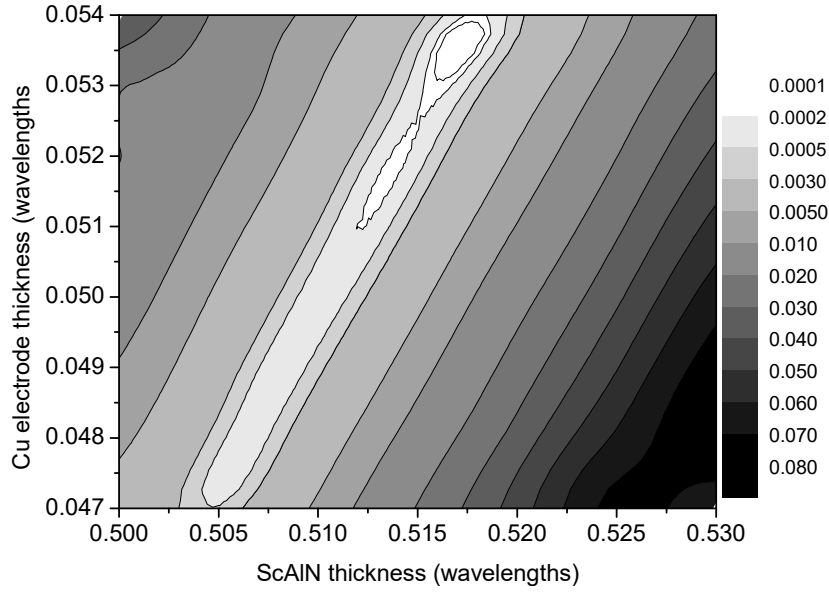


Fig. 5. Attenuation of the high velocity leaky SAW in dB/λ estimated at resonant frequency in Sc_{0.4}Al_{0.6}N/Sapphire with Cu grating, as a function of ScAlN and Cu electrode thicknesses.

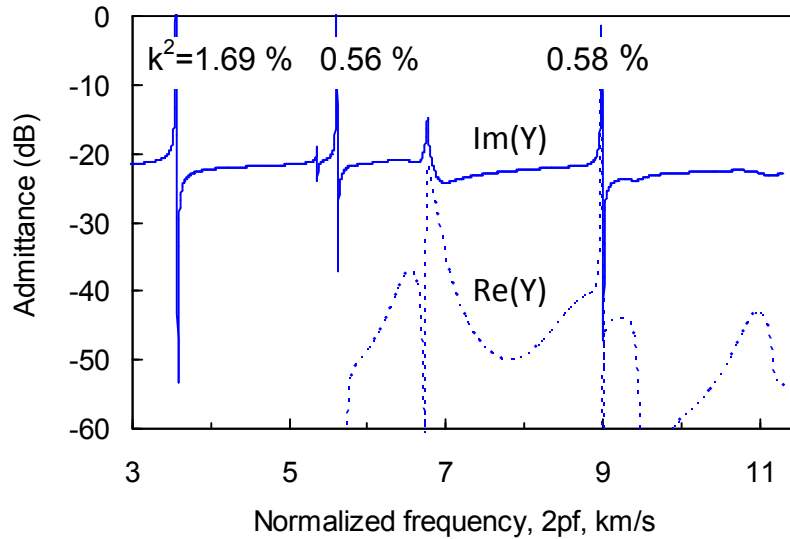


Fig. 6. Real and imaginary parts of admittance obtained numerically for Sc_{0.4}Al_{0.6}N/Sapphire with Cu grating. The thicknesses of ScAlN film and Cu electrodes are $h_f=0.515 \lambda$, and $h_{Cu}=0.05 \lambda$, respectively.

The use of dense Au electrodes leads to the increase of both velocity and k^2 of the longitudinal mode, as demonstrated in Fig. 7. The simulated admittance refers to the structure with Au and film thicknesses optimized to minimize the attenuation of the high-velocity mode. An excellent combination between a velocity of 9824 m/s, a k^2 equal to 1.106 % and high Q-factors of 3800 and 1480 at resonance and anti-resonance, respectively, was obtained.

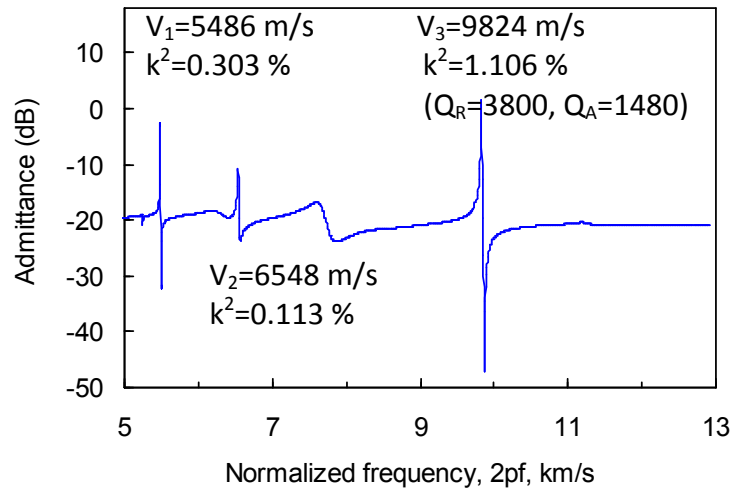


Fig. 7. Simulated admittance of resonator with Au electrodes on $\text{Sc}_{0.4}\text{Al}_{0.6}\text{N}/\text{Sapphire}$. The film and Au electrode thicknesses are $h_f=0.69 \lambda$, and $h_{\text{Au}}=0.005 \lambda$, respectively.

In summary, both $\text{Sc}_x\text{Al}_{1-x}\text{N}$ films and sapphire substrates are well adapted to high-temperature SAW applications, especially when x parameter is close to 0.1. When combined, $\text{Sc}_x\text{Al}_{1-x}\text{N}/\text{Sapphire}$ bilayer structure allows the generation of various modes, including leaky longitudinal high-velocity SAW. Theoretical investigations show that non-attenuated longitudinal SAW can propagate on the structure, provided a careful choice of the film thickness, as well as the electrode nature and thickness is made. The existence of such a mode is confirmed by the experimental investigation of SAW resonators based on highly-textured $\text{Sc}_{0.09}\text{Al}_{0.91}\text{N}$ films sputtered on sapphire substrates. These results pave the way for SAW multilayered structures based on ScAlN films dedicated to high-temperature applications, offering a unique combination between a large bandgap over 5 eV, a high SAW velocity near 10000 m/s and a k^2 above 1%.

Acknowledgments

This work was financially supported by the Lorraine Regional Council and the French National Research Agency (project “SALSA”, reference ANR-15-CE08-0015-05). It was also supported partly by the French PIA project “Lorraine Université d’Excellence”, reference ANR-15-IDEX-04-LUE and by the Ministry of Education and Science of the Russian Federation (Project 2.A03.21.0004/Grant K2-2016-072). Experiments were carried out on equipments part of IJL-TUBE Davm funded by FEDER(EU), PIA, region Grand Est, Metropole Grand Nancy and ICEEL. The authors wish to acknowledge H. Mishra for fruitful discussions.

References

- [1] M. Pereira da Cunha, Proc. IEEE Ultrason. Symp., 1337 (2013)
- [2] T. Kim, I. S. Didenko, J. Kim, R. Dalmau, R. Schlessler, E. Preble and X. Jiang, [IEEE Trans. Ultrason. Ferroelectr. Freq. Control](#) **62**, 1880 (2015).
- [3] T. Aubert, O. Elmazria, B. Assouar, L. Bouvot, and M. Oudich, [Appl. Phys. Lett](#) **96**, 203503 (2010).
- [4] T. Aubert, J. Bardong, O. Legrani, O. Elmazria, B. Assouar, G. Bruckner and A. Talbi, [J. Appl. Phys.](#) **114**, 014505 (2013).
- [5] C. Caliendo, [Appl. Phys. Lett.](#) **92**, 033505 (2008).
- [6] L. Reindl and W. Ruile, Proc. IEEE Ultrason. Symp., 125 (1993)
- [7] M. Akiyama, T. Kamohara, K. Kano, A. Teshigahara, Y. Takeuchi, and N. Kawahara, [Advanced Materials](#) **21**, 593 (2009).
- [8] H. Ichihashi, T. Yanagitani, M. Suzuki, S. Takayanagi, M. Matsukawa, Proc. IEEE Ultrason. Symp., 2521 (2014)
- [9] N. F. Naumenko and I. S. Didenko, [Appl. Phys. Lett](#) **75**, 3029 (1999).
- [10] R. Deng, S. R. Evans and D. Gall, , [Appl. Phys. Lett](#) **102**, 112103 (2013).
- [11] I. S. Didenko, F. S. Hickernell, and N. F. Naumenko, [IEEE Trans. Ultrason. Ferroelectr. Freq. Control](#) **47**, 179 (2000).
- [12] A.N. Darinskii, I. S. Didenko, N. F. Naumenko, [J. Acoust. Soc. Amer.](#) **107**, 2351 (2000).
- [13] N. F. Naumenko, [J. Appl. Phys.](#) **116**, 104503 (2014)
- [14] S. Zhang, W. Y. Fu, D. Holec, C. J. Humphreys and M. A. Moram, [J. Appl. Phys.](#) **114**, 243516 (2013).
- [15] N. F. Naumenko, [Ultrasonics](#) **95**, 1 (2019).